TRENDS IN SCIENCES 2026; 23(12): 14056
https://doi.org/10.48048/tis.2026.14056
RESEARCH ARTICLE

High-Temperature Activation-Induced Structural Evolution and Electrochemical Behavior of N-Doped Carbon from Coffee Waste

Arrak Klinbumrung[1], Reungruthai Sirirak[1], Santi Maensiri[2] and Tanissara Pinijmontree[3,*]

[1]*School of Science, University of Phayao, Phayao 56000, Thailand*
[2]*SUT Center of Excellence on Advanced Functional Materials, Suranaree University of Technology, Nakhon Ratchasima 30000, Thailand*
[3]*Faculty of Science and Agricultural Technology, Rajamangala University of Technology Lanna, Tak 63000, Thailand*

([*]Corresponding author's e-mail: tanissara_p@rmutl.ac.th; arassinat@gmail.com)

Received: 11 April 2026, Revised: 13 May 2026, Accepted: 20 May 2026, Published: 15 July 2026

Abstract

This study reveals that N-doping significantly enhances surface polarity, making coffee-derived carbon a competitive candidate for supercapacitors. Nitrogen-doped activated carbons were synthesized from waste coffee grounds through chemical activation using KOH and $ZnCl_2$ at 800 and 900 °C. The effects of activation temperature and chemical agents on the structural, textural, and electrochemical properties were systematically investigated. Increasing activation temperature promoted graphitization and optimized the micro-mesoporous hierarchy. Nitrogen doping introduced abundant pyridinic- and graphitic-N sites, enhancing surface polarity and electrical conductivity. Among all samples, the 900 °C-activated and N-doped sample exhibited the highest BET surface area (1,250 m^2/g) and a well-developed pore network, resulting in a superior specific capacitance of 241 F/g and 99% retention after 1,000 charge-discharge cycles. XPS analysis confirmed the dominance of pyridinic and graphitic nitrogen species, which enhanced electrical conductivity and ion accessibility. The combined effects of nitrogen doping and optimized activation conditions led to higher energy density and rate capability, demonstrating the potential of biomass-derived carbons for high-performance supercapacitors. The study provides a scalable and eco-efficient strategy for valorizing coffee waste into energy storage materials, contributing to clean energy, innovation and infrastructure, and responsible production and consumption.

Keywords: Waste coffee ground, Nitrogen dopant, Thermal activation, Structural evolution, Activated carbons, Electrochemical properties

Introduction

The rise in global energy demand and the depletion of fossil resources have created an urgent need for sustainable, clean, and efficient energy storage technologies. The rapid transition toward renewable energy systems, such as solar, wind, and biomass, necessitates reliable storage devices capable of buffering energy fluctuations and delivering high power density. Among available technologies, electrochemical capacitors have attracted significant interest due to their superior power performance, long cycling life, and environmental compatibility, making them promising for hybrid electric vehicles and portable electronics [1-3].

In recent years, biomass-derived carbon materials have gained attention as optical-sensing detection and sustainable electrode materials for electrochemical energy storage due to their natural abundance, cost-effectiveness, and intrinsic heteroatom content [4-6]. Moreover, the global abundance and zero-cost nature of coffee waste make it a highly attractive precursor for large-scale carbon material synthesis. Especially, spent coffee grounds were chosen due to their inherent

nitrogen-rich and high carbon density, which simplify the doping process. Based on its straightforward chemical activation, this synthesis approach provides great potential for pilot-scale manufacturing, even though it is currently employed at the laboratory scale. Biomass precursors of coconut shells, rice husks, and coffee grounds contain high carbon fractions and oxygen- or nitrogen-containing functional groups. These heteroatoms can facilitate doping and activation. The valorization of biomass waste into high-value carbon materials also contributes to environmental protection and the circular economy [7]. Among biomass waste, waste coffee grounds are particularly promising because of their uniform particle size, high carbon content of about 50 - 55 wt%, and inherent nitrogen species, making them ideal for synthesizing nitrogen-doped activated carbons [8]. Activated carbons remain the most common electrodes for electric double-layer capacitors due to their tunable porosity and high chemical stability [9,10]. However, conventional carbons often lack sufficient pseudo-capacitance. Recent research has shown that heteroatom doping, particularly with nitrogen, can significantly enhance electrochemical performance by improving wettability, conductivity, and charge-storage capacity [11,12]. Nitrogen atoms incorporated into the carbon framework generate various functional groups, including pyridinic-N, pyrrolic-N, and quaternary-N. These groups modulate the electronic structure and create redox-active sites, improving charge transfer [13].

Chemical activation plays a crucial role in developing the pore architecture of activated carbons. Among activation agents, KOH and $ZnCl_2$ are the most intensively researched used due to their effectiveness in producing high surface area and hierarchical porosity. KOH activation generally results in extensive micro- and mesopore networks, enhancing ion transport and electrolyte accessibility [14,15]. In contrast, $ZnCl_2$ activation promotes dehydration and crosslinking reactions, leading to higher nitrogen retention and micropore formation, often resulting in a lower overall surface area [16]. Several studies have demonstrated that the synergistic combination of chemical activation and nitrogen doping can simultaneously optimize surface area, pore structure, and surface functionality, improving energy and power densities [17,18]. Nevertheless, the effect of activation temperature remains inadequately understood. Temperature controls the decomposition of activating agents, the formation of volatile intermediates (for instance, K_2CO_3, CO_2), and the stability of nitrogen on the carbon framework [18,19]. Excessive activation temperature (more than 900 °C) can collapse micropores and destroy nitrogen functionalities, while lower temperatures may limit pore development. Hence, understanding how temperature affects the evolution of both textural and surface chemistry during activation is essential for optimizing electrochemical performance [20,21]. Despite growing interest in biomass-derived activated carbons, few studies have conducted a comparative evaluation of KOH- and $ZnCl_2$-activated systems derived from the same precursor under different activation temperatures. Most existing studies focus on a single activating agent or a specific temperature, providing partial insights into the structure-performance relationship. Moreover, the combined effect of activation route and post-synthetic nitrogen doping on the resulting electrochemical properties remains underexplored.

To address the gap, this work aims to elucidate the influence of activation temperatures of 800 and 900 °C on the microstructural, surface chemical, and electrochemical characteristics of nitrogen-doped activated carbons derived from waste coffee grounds. By employing KOH and $ZnCl_2$ as activation agents and subsequently nitrogen-doping, the study investigates the effect of thermal conditions on the interplay among specific surface area, pore structure, heteroatom functionality, and electrochemical performance. A comprehensive characterization using BET, Raman, XRD, SEM, and XPS is conducted to correlate physical and chemical properties with charge-storage behavior. The study provides insight into the temperature-activation relationship in dual-activated carbons and demonstrates that a controlled balance between porosity and nitrogen functionalization enhances supercapacitor performance. The novelty lies in the comparative activation of KOH and $ZnCl_2$ under the same conditions, and in the analysis of temperature effects on nitrogen incorporation and pore development. The results establish fundamental guidelines for designing sustainable, high-performance biomass-derived electrodes for next-generation electrochemical energy storage devices.

Materials and methods

Synthesis of N-doped activated carbon materials

To maintain uniformity of biomass precursor, a single batch of spent coffee grounds were collected from single supplier and ensuring a consistent batch for all experiments. The preparation conditions of the nitrogen-doped activated carbon samples are summarized in **Table 1**. Dried coffee grounds were mixed with either 10 wt% $ZnCl_2$ or 10 wt% KOH as activating agents at a material-to-liquor ratio of 1:4 by weight. The mixtures were placed in alumina crucibles and heated at a rate of 5 °C min^{-1} from room temperature to 800 or 900 °C for 1 h under a continuous nitrogen flow and then cooled naturally to room temperature. The carbonized products were washed with 0.6 M HCl to remove residual inorganic salts, then rinsed with distilled water until the solution reached neutral pH, pH 7. Finally, the prepared carbons were dried at 100 °C until a constant weight was reached (approx. 2 h) to ensure complete dehydration, then stored in a desiccator for further use [22,23]. Nitrogen doping was conducted by soaking the activated carbons in 37% nitric acid at 60 °C for 2 h, followed by thorough washing and drying at 60 °C. Finally, the dried N-doped activated carbon samples were annealed in nitrogen at 600 °C for 2 h to remove surface oxygen groups and stabilize nitrogen functionalities [24].

Table 1 Sample name and preparation process.

Sample Name	Activating Reagent	Activating Temperature
CFN8	-	800 °C
CKN8	KOH	800 °C
CZN8	$ZnCl_2$	800 °C
CFN9	-	900 °C
CKN9	KOH	900 °C
CZN9	$ZnCl_2$	900 °C

Materials characterizations

The microstructural characteristics of the synthesized carbon materials were examined using X-ray diffraction (XRD, Bruker D2 Phaser). Raman spectroscopy (JOBIN YVON HORIBA, T64000) was employed to identify the structural disorder and surface functional groups of the carbons. Nitrogen adsorption-desorption isotherms were measured with a BELSORP mini II analyzer to determine specific surface area and pore-size distribution. The obtained data were evaluated using the Brunauer-Emmett-Teller (BET), Barrett-Joyner-Halenda (BJH), and Brunauer's MP methods. The surface morphology was observed with a field-emission scanning electron microscope (FESEM, JEOL JSM-7800X). In addition, X-ray photoelectron spectroscopy (XPS) was performed to analyze surface elemental composition and bonding states, providing insight into the relationship between the microstructural features and the electrochemical behavior of the activated carbons.

Electrochemical measurements

The electrochemical performance of the prepared carbon materials was evaluated using a 3-electrode cell configuration at room temperature in an aqueous electrolyte. A platinum wire and an Ag/AgCl electrode served as the counter and reference electrodes, respectively. The working electrode was prepared by mixing N-doped activated carbon (80 wt%) with polyvinylidene fluoride (PVDF, 10 wt%) and carbon black (10 wt%) in N-methyl-2-pyrrolidinone (NMP) to form a homogeneous slurry. The mixture was uniformly coated onto a nickel foam substrate (1 cm^2) and dried at 60 °C for 24 h. Before testing, the electrode was immersed in a 6 M KOH solution for 8 h to ensure complete electrolyte penetration.

Electrochemical measurements were carried out using a Metrohm Autolab model PGSTAT302N potentiostat/galvanostat. Cyclic voltammetry (CV) and galvanostatic charge-discharge (GCD) tests were performed to assess the capacitive behavior of the electrodes. Electrochemical impedance spectroscopy (EIS) was conducted. The specific capacitance (C_s),

energy density (E), and power density (P) were calculated from the electrochemical data following standard equations [25,26].

Results and discussion

The crystallographic structure of the synthesized nitrogen-doped activated carbons was examined using X-ray diffraction (XRD). The corresponding diffraction patterns are shown in **Figure 1**. All samples exhibit 2 broad peaks centered at 2θ of 24° - 26° and 43°, corresponding to the (002) and (100) planes of turbostratic carbon, respectively. The broad, low-intensity (002) peaks confirm the principally amorphous nature of the carbons, consistent with biomass-derived materials activated at moderate temperatures [27]. A shift of the (002) peak toward higher 2θ values with increasing activation temperature indicates partial ordering of the carbon structure. According to Bragg's law, a shift of the (002) peak toward higher 2θ values indicates a decrease in interlayer spacing, suggesting closer stacking of carbon layers and partial recovery of graphitic ordering at higher activation temperatures. Samples activated at 900 °C show slightly sharper (002) peaks compared to those treated at 800 °C, suggesting enhanced structural rearrangement and increased graphitic domain size. In accordance with the report of Yuan *et al.* [28], higher activation temperatures promote carbon atom rearrangement and removal of disordered amorphous phases, resulting in a more ordered turbostratic structure.

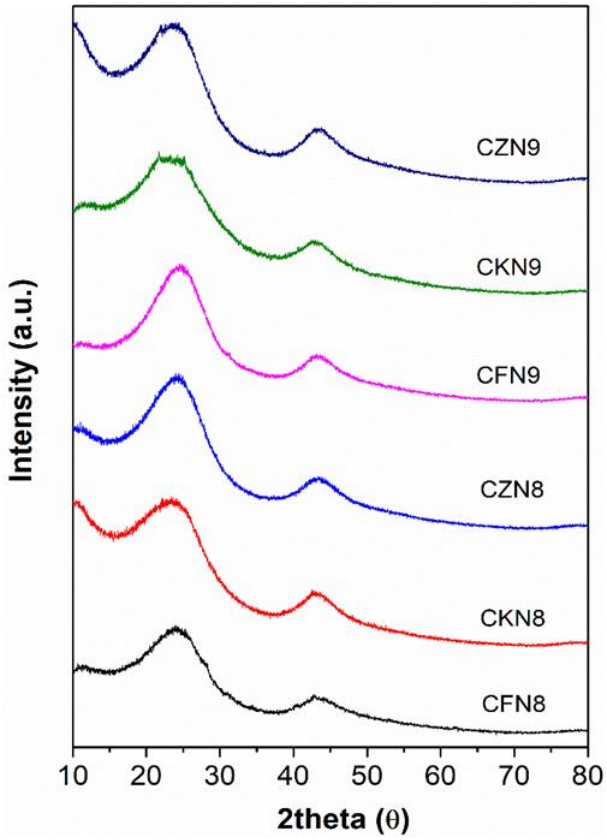


Figure 1 XRD scattering patterns of as-synthesized N-doped activated carbons derived from spent coffee grounds, activated at 800 and 900 °C

The samples activated with KOH displayed broader (002) peaks than those activated with $ZnCl_2$, indicating a higher degree of structural disorder. The difference can be attributed to the stronger etching and gasification effects of KOH during activation, which create more micropores and defects within the carbon matrix [5,29]. Conversely, $ZnCl_2$ activation produces minor dehydrogenation and crosslinking reactions, favoring the formation of more compact carbon domains with lower structural distortion [19]. The findings result from the aggressive redox reaction between KOH and carbon, whereas $ZnCl_2$ promotes dehydration and

crosslinking, with less severe lattice disruption. Nitrogen doping and subsequent annealing slightly affected the materials' crystallinity. The appearance of (002) crystal plane in N-doped samples implies that nitrogen incorporation introduced lattice defects and expanded interlayer spacing due to substitutional or pyridinic-type nitrogen atoms within the carbon lattice [30]. Similar behavior was observed by Yuan *et al.* [28], who reported that nitrogen doping in coffee-ground-derived carbons increased interlayer spacing, thereby facilitating ion diffusion and charge storage performance.

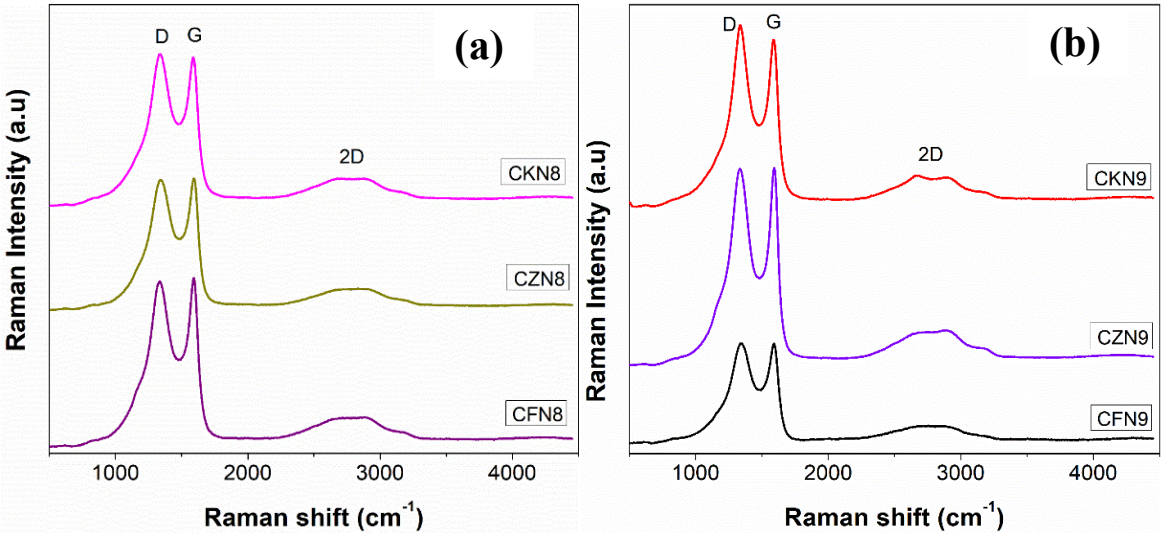


Figure 2 Raman spectra of as-synthesized N-doped activated carbon derived from waste-grounded coffee, activated at (a) 800 and (b) 900 °C

To further investigate the structural evolution and the degree of disorder within the carbon framework, Raman spectroscopy was employed. **Figure 2** illustrates the Raman spectra of the N-doped activated carbons synthesized at 800 and 900 °C. As shown in **Figure 2**, Raman spectroscopy was employed to evaluate the structural disorder and degree of graphitization of the prepared nitrogen-doped activated carbons. The spectra of the samples activated at 800 and 900 °C are shown in **Figures 2(a)** and **2(b)**. All spectra exhibit 2 distinct bands at 1,345 and 1,585 cm^{-1}, assigned to the D and G bands, respectively. The D band corresponds to the vibration of sp^3-bonded carbon atoms at lattice defects, while the G band originates from the in-plane stretching of sp^2-bonded carbon in graphitic domains [19,31]. The D band arises from disorder-induced breathing modes of sp^3 carbon rings and becomes Raman-active in the presence of defects, edges, and vacancies of distorted carbon sites. Therefore, a stronger D band indicates increased structural disorder in the carbon framework. Besides, the 2D band of the graphitic carbon material was observed at 2,882 cm^{-1}. The broad 2D band is a second-order overtone of the D band, reflecting stacking and layering interactions in graphitic carbon [32].

The relative intensity ratio (I_D/I_G) is used to assess the degree of disorder within carbon materials [33]. In this study, the I_D/I_G ratio slightly decreased with increasing activation temperature from 800 to 900 °C, implying an enhancement of graphitic ordering and partial recovery of sp^2 domains [34]. This trend indicates that elevated activation temperatures promote the rearrangement of carbon layers and reduce amorphous defects in coffee-derived carbons [28]. Differences between activation agents were also manifest. KOH-activated samples exhibited higher I_D/I_G ratios than those activated with $ZnCl_2$, indicating a higher defect density and smaller crystalline domains. The strong redox and gasification reactions associated with KOH activation produce extensive microporosity and disturb graphitic layers. While $ZnCl_2$ activation favors cross-linking and dehydration, yielding more ordered carbon frameworks [5,35]. In correspondence with previous reports, activation chemistry influences the structural evolution of coffee-waste carbons [27].

Nitrogen doping further affected the Raman spectrum. The D band intensity increased slightly with sample doping, suggesting the incorporation of nitrogen atoms into the carbon lattice. The finding introduces lattice strain and additional edge defects [30]. The shift of the G band toward lower wavenumbers indicates electron-donating effects of nitrogen atoms on the π-electron system, consistent with XPS observations of pyridinic- and graphitic-N species. Structural features enhance electrical conductivity and provide abundant electrochemically active sites, thereby benefiting charge storage processes [36]. Pyridinic-N provides electrochemically active edge sites and increases surface polarity, while graphitic-N enhances electron delocalization within the sp^2 carbon network. Together, these structural features improve conductivity, wettability, and charge-storage kinetics.

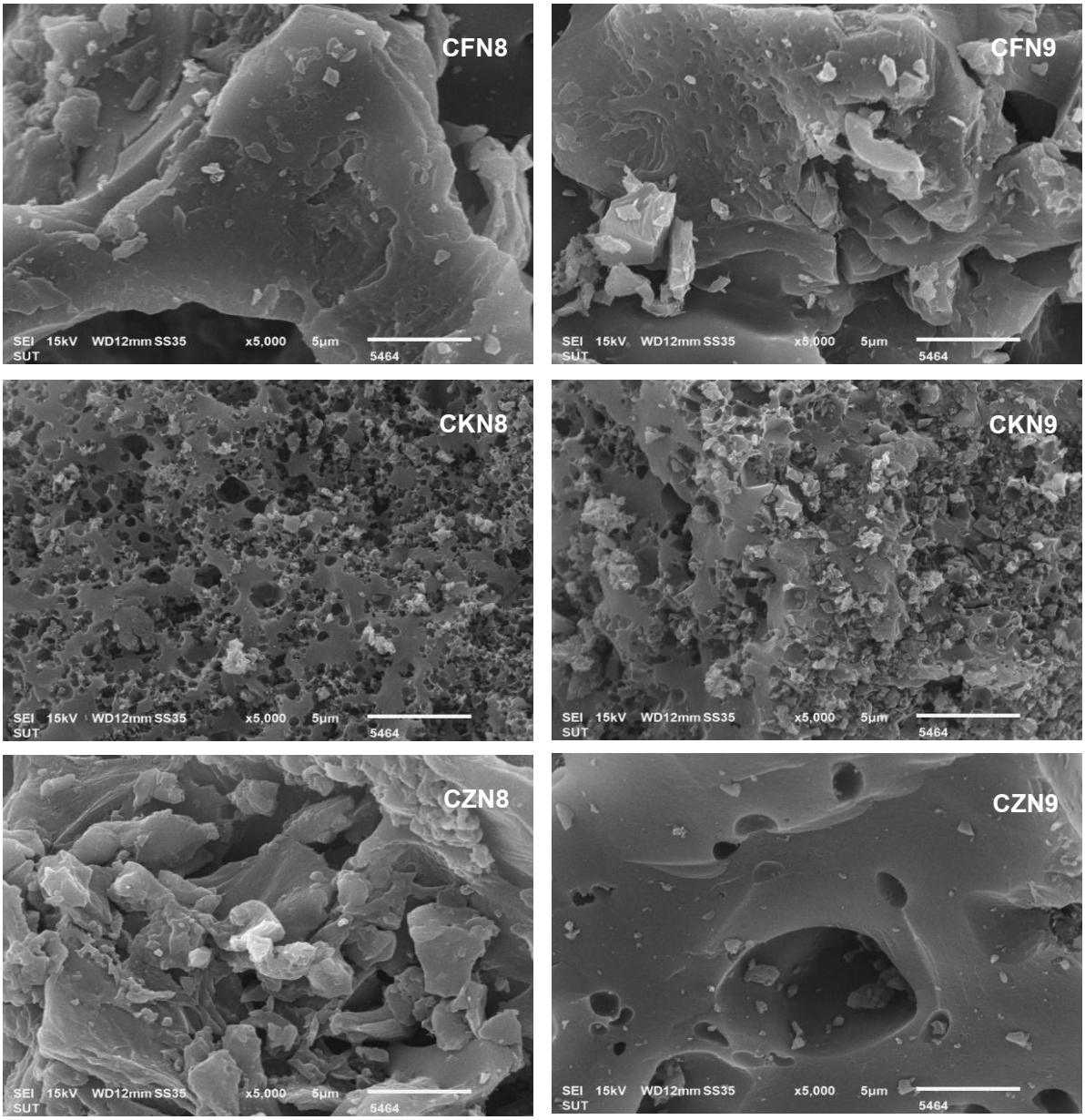


Figure 3 Surface morphology of as-synthesized N-doped activated carbon derived from waste-grounded coffee, activated at 800 and 900 °C

To visualize the impact of activation temperature on the development of porous structures and surface characteristics, Scanning Electron Microscopy (SEM) was employed. The surface morphologies of the nitrogen-doped activated carbons obtained at different activation temperatures and with different activating

agents are shown in **Figure 3**. The SEM images represent the typical surface morphology observed across multiple scanned areas. All micrographs reveal that all samples exhibit irregular porous morphology of activated carbons derived from biomass precursors. Numerous pores and cavities are observed across the particle surfaces, which can be attributed to the release of volatile gases and the decomposition of organic components during carbonization and activation [4,19]. As mentioned above, the irregular porous morphology can be attributed to the heterogeneous composition of coffee waste, including cellulose, hemicellulose, lignin, proteins, and minerals. The uneven decomposition during carbonization releases volatile gases that generate cavities and interconnected pores.

A comparative morphological assessment reveals a clear evolution of the surface structure as a function of temperature. At a lower activation temperature of 800 °C, the samples exhibit a relatively compact and dense morphology with isolated, smaller pores. In contrast, increasing the temperature to 900 °C results in a significantly more developed and open-textured framework. This suggests that higher thermal energy promotes extensive chemical etching, leading to the formation of an interconnected network of pore channels. This morphological shift—from a compact state to a highly porous structure—is consistent with the gasification reactions that facilitate the transformation of micropores into larger mesoporous structures, as further confirmed by the nitrogen physisorption results [28].

The activating agent had a pronounced influence on surface morphology. KOH-activated carbons showed highly fractured surfaces with irregular pore distribution, reflecting the strong etching and redox activity of KOH with carbon. During activation, KOH decomposes into K_2CO_3 and metallic K, which are incorporated into the carbon lattice, generating numerous micropores [35]. In contrast, $ZnCl_2$-activated carbons exhibited more uniform compact pore structures. These are consistent with its mild dehydration and crosslinking mechanism, which organize the formation of mesoporous structures with higher structural integrity [37]. In agreement with a prior study, $ZnCl_2$-assisted activation of coffee waste yielded more solid-pore structures than KOH activation [27]. Because of the uniform pore structure, it can be concluded that $ZnCl_2$-activated carbons suppress excessive carbon burn-off and preserve a more compact framework with relatively homogeneous pore formation.

Nitrogen doping altered the surface texture, producing more defect-rich and slightly rougher surfaces. The acid treatment introduced new active sites and oxygen-nitrogen functional groups, thereby improving hydrophilicity and enhancing the accessibility of electrolyte ions to the pore network [28]. These features are advantageous for electrochemical energy storage because the hierarchical pore system and heteroatom-induced defects facilitate ion transport, reduce diffusion distances, and improve charge storage at the electrode-electrolyte interface [38].

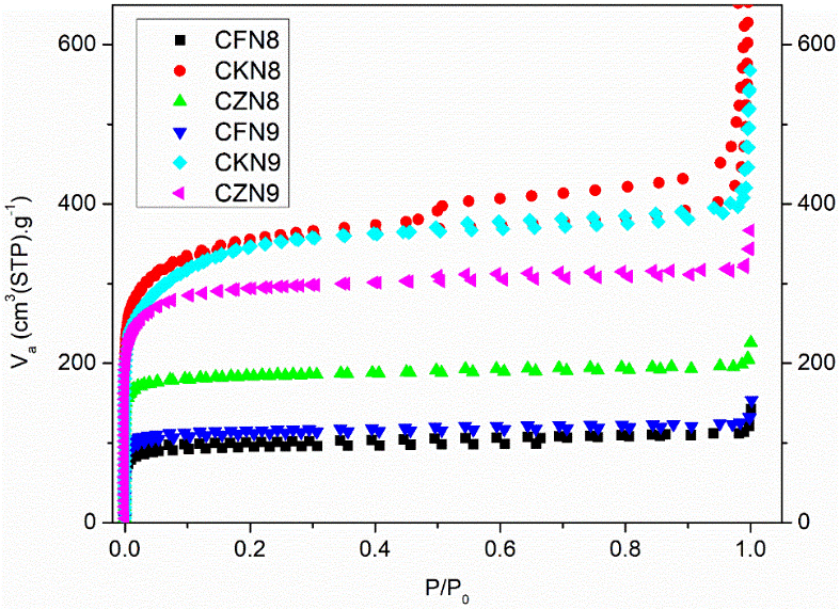


Figure 4 Nitrogen adsorption/desorption isotherms of as-synthesized N-doped activated carbons derived from waste-grounded coffee, activated at 800 and 900 °C.

Table 2 Specific surface areas and pore volume of N-doped activated carbons.

Sample name	BET surface area (m^2/g)	Pore volume (cm^3/g)
CFN8	-	-
CKN8	1160	0.736
CZN8	591	0.312
CFN9	436	0.200
CKN9	1250	0.637
CZN9	1130	0.496

As presented in **Figure 4** and **Table 2**, the nitrogen adsorption-desorption isotherms and BET data show that all nitrogen-doped activated carbons display type I isotherms with distinct hysteresis loops, indicating combined micro- and mesoporosity [4]. A sharp rise at low relative pressure ($P/P_0 < 0.1$) confirms micropore formation, while gradual adsorption at higher pressures reflects mesopore development. Activation temperature and reagent significantly influenced the textural parameters. The KOH-activated carbons exhibited the highest surface areas and pore volumes, showing CKN8 (1160 m^2/g, 0.736 cm^3/g) and CKN9 (1250 m^2/g, 0.637 cm^3/g). Whereas the $ZnCl_2$-activated samples show values of 591 m^2/g and 0.312 cm^3/g for CZN8, and 1130 m^2/g and 0.496 cm^3/g for CZN9. The high surface area and pore volume of KOH-activated carbons result from the reaction of KOH with carbon, producing the species of K_2CO_3, CO, CO_2, H_2, and metallic K. These species diffuse into the carbon framework and expand the carbon layers, generating abundant micro- and mesopores. The non-activated carbons showed minimal porosity, confirming that chemical activation is essential for structural development. Higher temperature enhanced efficiency by accelerating gasification and opening closed pores. Temperature activation increases the surface area of coffee-waste-derived carbons [28]. The superior porosity of KOH-activated samples arises from strong redox reactions that generate gaseous byproducts, including CO, CO_2, and H_2, thereby creating abundant micropores [8]. In contrast, $ZnCl_2$ promotes lower dehydration and crosslinking reactions, producing mesoporous carbons with smoother surfaces and lower overall surface area [39]. Nitrogen doping slightly reduced the total surface area but improved mesoporosity and surface wettability, facilitating ion diffusion and electrolyte penetration. Decreasing

surface area after nitrogen doping may result from partial occupation of micropores by nitrogen- and oxygen-containing groups. These polar groups improve electrolyte wettability and facilitate ion transport through accessible mesoporous channels. As a result, CKN9 exhibited the most favorable textural properties, combining high surface area and balanced micro–mesoporosity, suggesting enhanced capacitive behavior in subsequent electrochemical testing.

The electrochemical performance of the nitrogen-doped activated carbon electrodes was evaluated using galvanostatic charge-discharge (GCD). As displayed in Fig. 6, all samples exhibited nearly symmetrical triangular profiles, confirming the ideal capacitive behavior and high reversibility typical of electric double-layer capacitors (EDLCs) [40]. Among the samples, CKN9 provided the longest discharge time, indicating the highest specific capacitance. This can be attributed to its high BET surface area (1,250 m^2/g) and hierarchical pore distribution, which facilitate rapid ion transport and efficient electrolyte diffusion. The CKN8 and CZN9 electrodes also exhibited moderate discharge times. CFN8 and CFN9 showed lower performance due to their limited porosity and fewer electroactive sites. Similar correlations between surface area and capacitance have been reported for coffee-waste-derived carbons activated by KOH and $ZnCl_2$ [8,39].

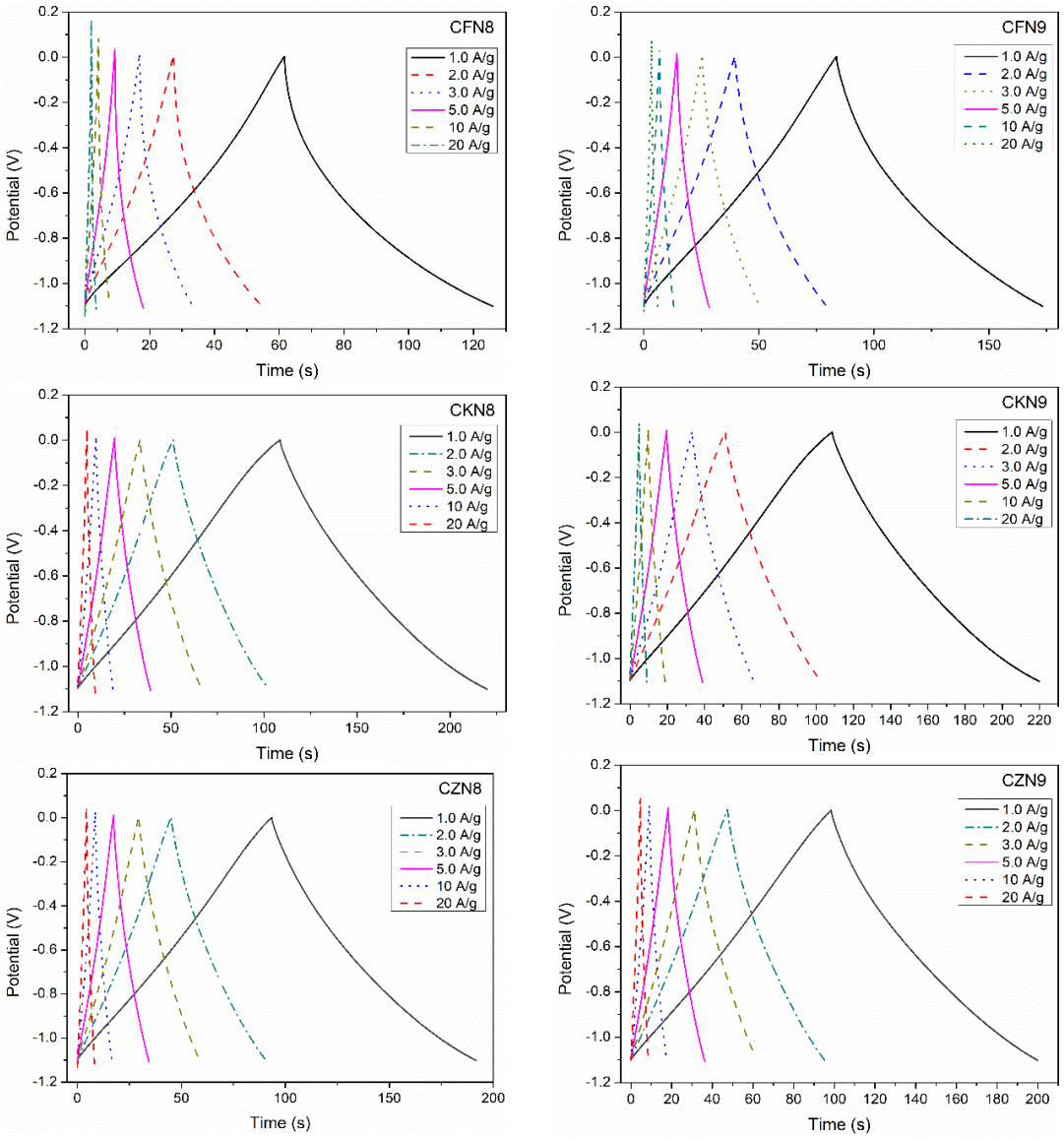


Figure 5 GCD curves of N-doped activated carbon electrode derived from waste coffee grounds at various energy densities.

The cyclic voltammetry (CV) curves of the nitrogen-doped activated carbons are illustrated in **Figure 6**. The specific capacitance data are summarized in **Table 3**. All samples exhibited quasi-rectangular CV profiles without distinct redox peaks, confirming that the capacitance behavior is primarily governed by electric double-layer capacitance (EDLC) [4]. The slight humps observed in CKN9 and CZN9 suggest minor pseudocapacitive contributions from nitrogen- and oxygen-related surface functionalities [41]. The curve area, interpreted as stored charge, increased significantly with activation temperature and activating agent. CKN9 displayed the largest enclosed area and the most ideal rectangular shape. The largest enclosed CV area indicates the highest charge-storage capacity, while its nearly rectangular shape reflects rapid ion adsorption/desorption, low polarization, good electrical conductivity, and efficient electrolyte access within the hierarchical porous structure. In contrast, CFN8 and CFN9 exhibited narrower curves, reflecting limited ion accessibility and low capacitance. Similar trends have been reported for KOH- and $ZnCl_2$-activated coffee-waste carbons, where enhanced porosity and heteroatom doping improved capacitance and rate response [5].

The specific capacitance (C_s) of the prepared materials can be determined using the following equation [42].

$$C_s = \frac{Q}{2\Delta V} = \frac{1}{2mv(V_c - V_a)} \int_{V_a}^{V_c} I(V)dV \quad (1)$$

where C_s is the specific capacitance (F/g), Q is the charge obtained by integrating the area under the CV curves, m denotes the active material mass in the electrode (g), ν is the potential scan rate (mV/s), $\Delta V = Vc - Va$ specifies the potential range for each CV measurement (−0.1 to 0.9 V vs. Ag/AgCl), and I(V) indicates the current response along the CV curve.

At low scan rates of 5 mV/s, the electrolyte ions can fully penetrate both micropores and mesopores, yielding a near-theoretical capacitance. The specific capacitances derived from the CV curves followed the sequence: CKN9 (241 F/g) > CZN9 (198 F/g) > CKN8 (176 F/g) > CZN8 (150 F/g) > CFN9 (110 F/g) > CFN8 (78 F/g). The high capacitance of CKN9 results from the synergistic effects of nitrogen doping and optimized pore connectivity, which together enhance electrolyte ion diffusion and surface redox activity [43]. Increasing scan rates, all samples maintained well-preserved CV shapes, indicating fast charge propagation and robust electrochemical stability [1].

At a scan rate of 10 mV/s, the CV profile provides a representative balance between the electric double-layer charging process and electrolyte ion diffusion through the porous carbon structure. The typical CV curves in **Figure 7** exhibit a large area, indicating a strong capacitive response of the as-fabricated electrode. As depicted in **Figures 7(a)** and **7(b)**, the comparison shows an area difference for KOH-activated carbon, as shown in **Table 3**: CKN8 > CKN9 > CFN9 > CFN8, whereas the $ZnCl_2$ activation series shows CZN9 > CZN8 > CFN9 > CFN8. This indicates that KOH activation enhances capacitance by creating a pore structure. Conversely, N-doping improves the supercapacitor performance of $ZnCl_2$-activated carbon materials at higher activation temperatures. The nitrogen-doped carbon material exhibits high electronegativity and electronic conductivity, as well as enhanced carbon surface wettability [44]. It also found that the doped atoms can defend against undesirable chemical reactions [45].

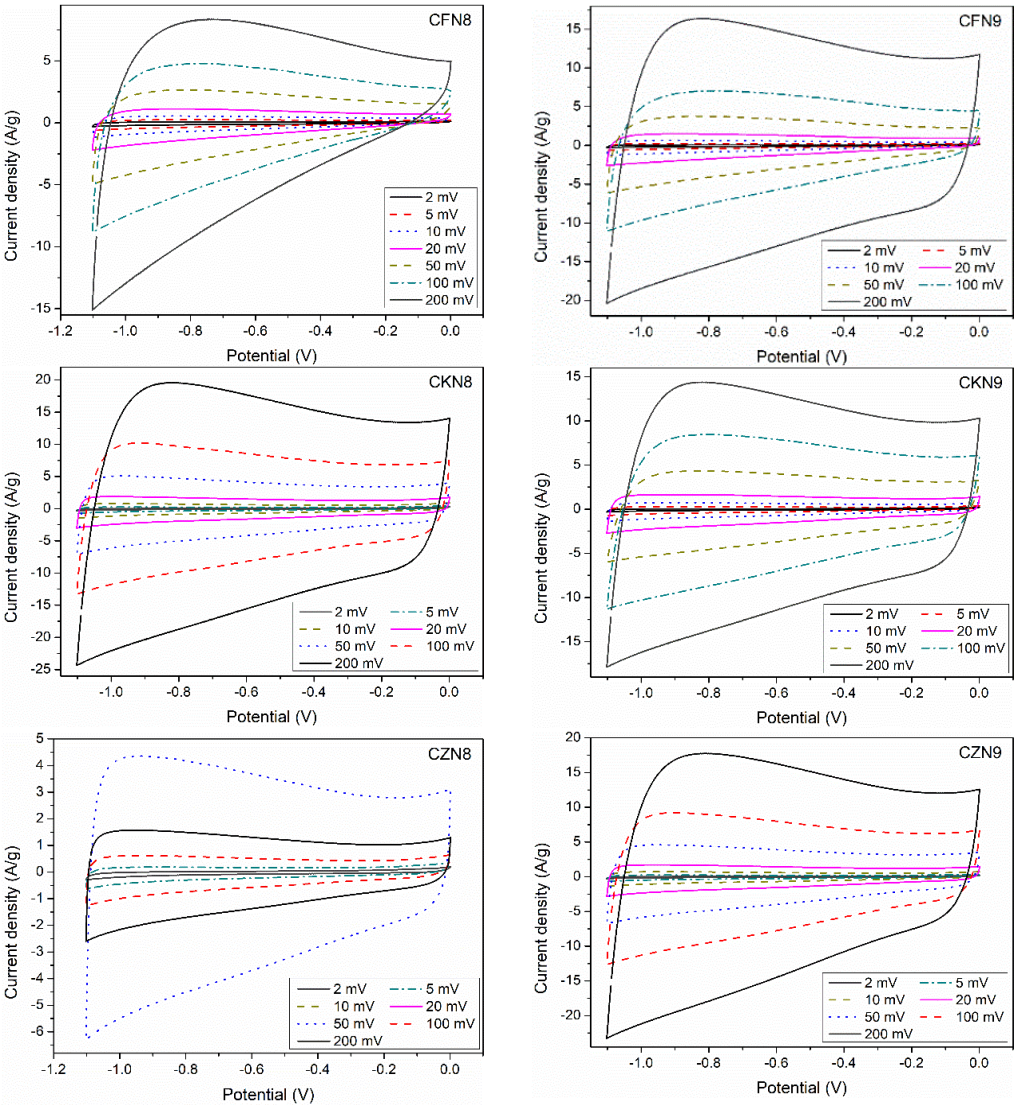


Figure 6 CV curve of N-doped activated carbon electrode derived from waste coffee grounds at various scan rates.

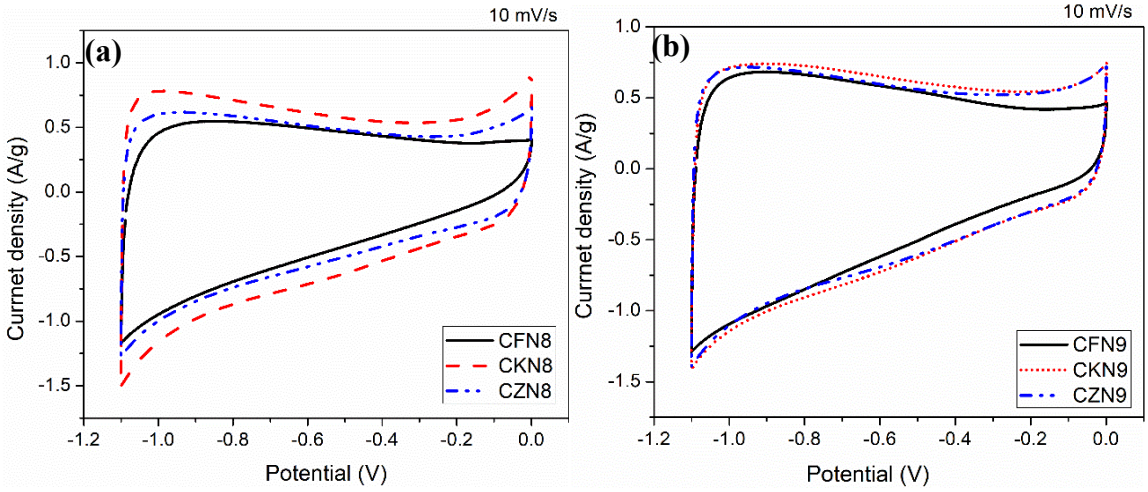


Figure 7 CV curve of N-doped activated carbon electrode at a scan rate of 10mV/s, activated at (a) 800 and (b) 900 °C.

Table 3 The specific capacitance (C_s), energy density (E), and power density (P) of N-doped activated carbon materials at various current densities.

Sample Name	Current (A/g)	C_s (F/g)	E (mWh/g)	P (mW/g)
CFN8	1	59.076	35.048	0.545
	2	50.390	29.581	1.084
	3	46.045	26.607	1.612
	5	40.888	23.406	2.675
	10	34.210	19.471	5.335
	20	28.846	15.600	10.400
CKN8	1	101.712	60.732	0.546
	2	94.458	55.831	1.087
	3	91.740	53.904	1.626
	5	89.190	51.665	2.691
	10	86.281	47.988	5.273
	20	83.039	43.504	10.236
CZN8	1	89.551	53.842	0.548
	2	83.280	49.827	1.094
	3	46.649	27.714	1.635
	5	77.709	46.214	2.726
	10	74.223	43.654	5.423
	20	70.799	40.791	10.734
CFN9	1	81.816	49.117	0.548
	2	73.038	43.594	1.092
	3	69.033	41.068	1.636
	5	64.254	37.858	2.714
	10	57.815	33.782	5.405
	20	52.062	29.052	10.564
CKN9	1	90.839	54.110	0.546
	2	82.969	48.705	1.084
	3	80.038	46.634	1.619
	5	76.876	43.733	2.667
	10	73.160	39.996	5.228
	20	69.682	34.162	9.902
CZN9	1	92.530	55.505	0.548
	2	87.316	52.116	1.092
	3	85.036	50.364	1.632
	5	82.436	48.314	2.707
	10	79.103	45.133	5.341
	20	76.074	42.064	10.516

The energy density and power density of materials were determined using the following equations [46].

$$E = \frac{1}{2} C_{CD} \Delta V^2 \quad (2)$$

$$P = \frac{E}{\Delta t} \quad (3)$$

where E is energy density, C_{CD} is specific capacitance from CD technique, ΔV is potential window, P is power density, and Δt is duration time.

As shown in **Figure 8**, the Ragone plots illustrate the relationship between energy and power densities of all nitrogen-doped activated carbons. At the lowest power density of 10.2 mW/g, the CKN8 electrode achieved the highest energy density of 60.7 mWh/g, surpassing the other samples. This superior value can be attributed to its well-balanced micro-mesoporous architecture and high nitrogen doping, which facilitate efficient ion diffusion and charge storage [40]. In comparison, CZN9 and CKN9 delivered slightly lower energy densities of 56.4 and 53.7 mWh/g, respectively, due to differences in pore connectivity and nitrogen configuration. The CZN8 electrode exhibited moderate energy (49.8 mWh/g), while CFN8 and CFN9 recorded the lowest values (< 40 mWh/g), consistent with their lower surface areas and less accessible pores. The trend demonstrates that KOH activation at 800 °C provides an optimal balance between porosity and electrical conductivity, yielding superior energy output under high-power operation [39].

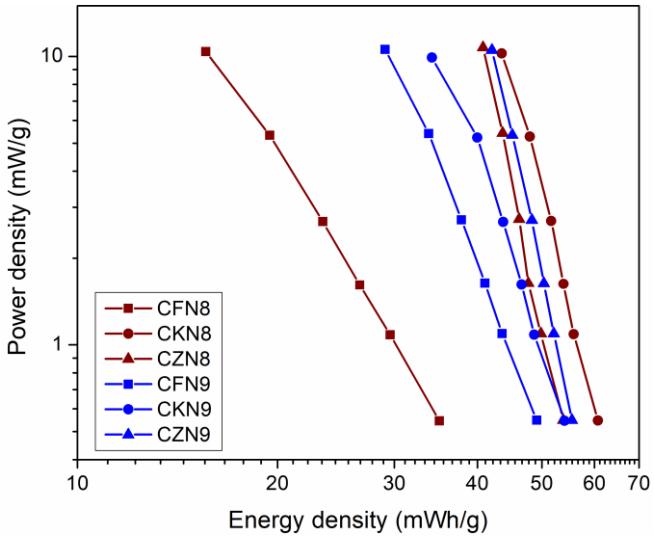


Figure 8 Ragone plots of various N-doped activated carbons.

Due to the interesting properties of CKN9, the cycling performance of the CKN9 electrode is illustrated in **Figure 9**. The capacitance remains constant at around 65 F/g over 1,000 continuous charge-discharge cycles, demonstrating excellent electrochemical reversibility and structural stability. The retention of 99% confirms the robustness of the porous framework and the strong adhesion of the active material to the current collector [40]. The synergistic effects of high surface area, hierarchical micro-mesoporosity, and nitrogen functionalities maintain effective ion diffusion and low internal resistance during prolonged cycling [5]. These results align with the superior rate and energy performance of CKN9 demonstrated in the preceding sections, confirming that optimized KOH activation and nitrogen doping enhance both capacitance and long-term durability.

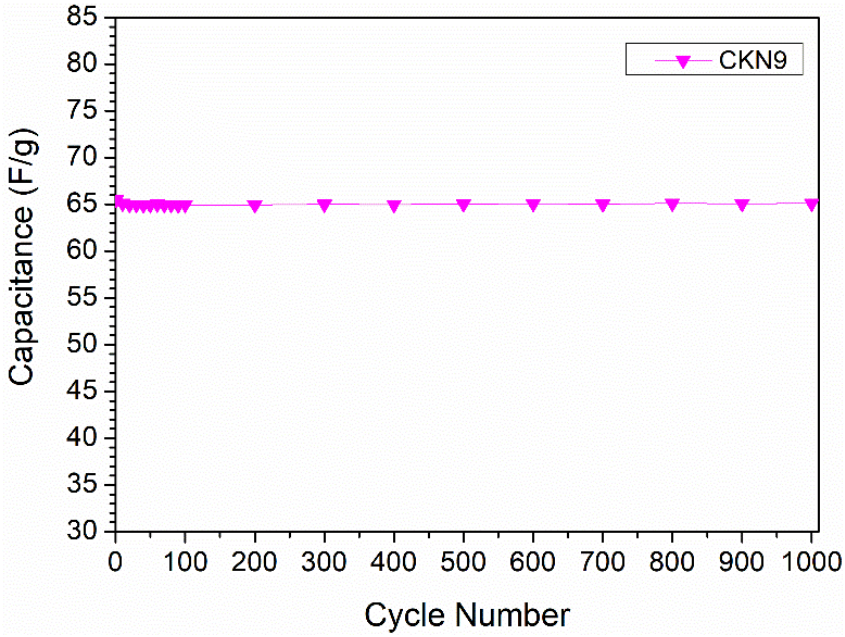


Figure 9 The capacity retention of the CKN9 electrode as a function of the charge-discharge cycle number.

The XPS spectra of the nitrogen-doped activated carbons activated at 800 and 900 °C are shown in **Figures 10** and **11**, respectively. The spectrum confirms the coexistence of carbon, nitrogen, and oxygen elements in all samples, validating successful nitrogen incorporation during the post-treatment process.

At 800 °C activation (**Figure 10**), the C 1s spectra display peaks centered around 284.6, 285.8, and 288.6 eV attributed to C–C/C=C, C–N, and C=O, respectively [28]. The N 1s spectra exhibit contributions from pyridinic-N (398.3 eV) and pyrrolic-N (400.2 eV) [28], while O 1 s spectra show features of C=O (531.6 eV) and O–C=O (533.2 eV) bonds [47]. These indicate partial surface oxidation and moderate nitrogen incorporation, typical of low-temperature activation [40]. On the contrary, at 900 °C (**Figure 11**), CKN9 and CZN9 reveal stronger C–N and graphitic-N peaks, suggesting conversion of unstable pyrrolic-N into more conductive graphitic-N species. The relative intensity of C=O decreases, reflecting oxygen removal and improved graphitization. This transformation enhances electronic conductivity and structural stability, directly correlating with the superior capacitance and cycling performance observed for CKN9 [39]. The slightly higher nitrogen content in CKN9 compared with CZN9 promotes improved charge transfer and wettability. These factors facilitate ion transport during electrochemical cycling. These XPS findings complement the BET and electrochemical results, confirming that high-temperature KOH activation effectively optimizes the chemical state and electronic structure of N-doped carbons, thereby enhancing capacitive behavior.

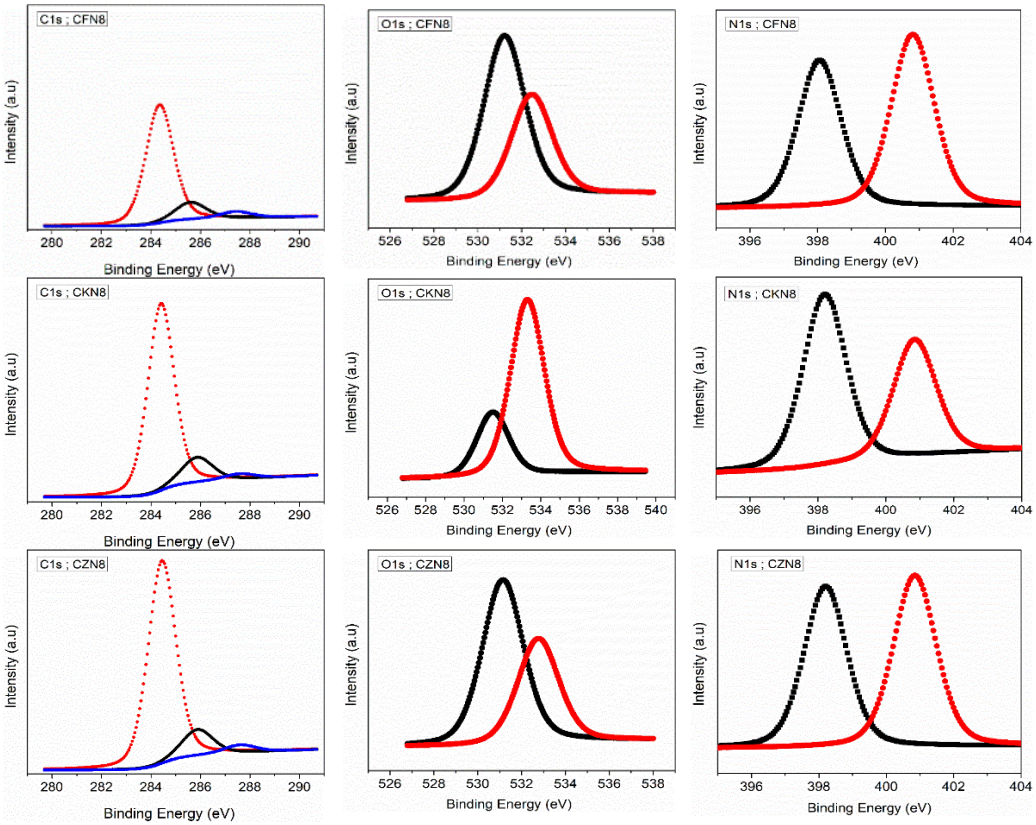


Figure 10 C1s, O1s, N1s XPS spectra of as-synthesized N-doped activated carbons derived from waste coffee grounds, activated at 800 °C.

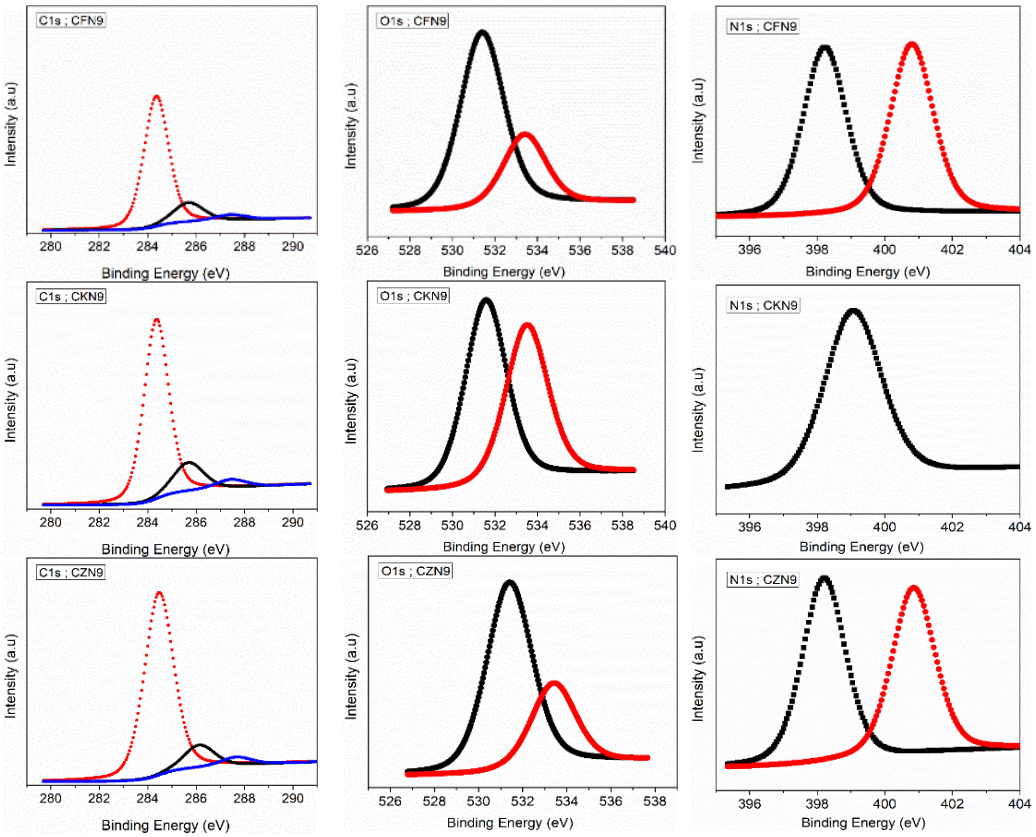


Figure 11 C1s, O1s, N1s XPS spectra of as-synthesized N-doped activated carbons derived from waste coffee grounds, activated at 900 °C.

Conclusions

Nitrogen-doped activated carbons were successfully synthesized from waste coffee grounds using KOH and $ZnCl_2$ as activating agents at 800 and 900 °C. The activation temperature and chemical agent were determined to be pivotal factors in regulating the pore structure, surface area, and nitrogen functionalities, which collectively influence electrochemical performance. Increasing the temperature from 800 to 900 °C promoted graphitization, reduced surface oxygen, and enhanced the formation of conductive pyridinic- and graphitic-N sites. Among all samples, CKN9 (KOH, 900 °C) showed the highest BET surface area (1,250 m^2/g), an optimal micro-mesoporous structure, and abundant nitrogen species, leading to a superior specific capacitance of 241 F/g, excellent rate capability, and 99% retention after 1,000 cycles. In contrast, $ZnCl_2$-activated and non-activated samples showed lower capacitance due to limited pore connectivity and lower heteroatom doping. The results confirm that high-temperature KOH activation effectively tailors the textural and electronic properties of biomass-derived carbons, enabling high-performance, durable, and sustainable electrodes for next-generation supercapacitors. This work demonstrates the potential of waste coffee grounds as a low-cost, environmentally friendly precursor for scalable energy storage materials.

Acknowledgements

This research was mainly supported by the Thailand Research Fund and Synchrotron Light Research Institute (SLRI), Grant No. TRG6080017. The partially supported by the University of Phayao and the Thailand Science Research and Innovation Fund (Fundamental Fund 2026, Grant No. 2273/2568). The authors thank Narong Chanlek (Ph.D.) from Synchrotron Light Research Institute (SLRI), Nakhon Ratchasima, Thailand, for their valuable assistance with the XPS analysis and sample preparation. We thank the School of Science, University of Phayao, Thailand for their general support of this work, and we extend our gratitude to the SUT Center of Excellence on Advanced Functional Materials, Suranaree University of Technology, and the Faculty of Science and Agricultural Technology, Rajamangala University of Technology Lanna, Tak, Thailand.

Declaration of Generative AI in Scientific Writing

The authors declare that this work is original and was created without the use of generative AI techniques. The authors were totally accountable for writing, data interpretation, and language corrections.

CRediT Author Statement

Arrak Klinbumrung: Writing - Reviewing and Editing; Validation; Visualization. **Reungruthai Sirirak**: Writing - Reviewing and Editing; Visualization. **Santi Maensiri**: Conceptualization; Resources. **Tanissara Pinijmontree**: Conceptualization; Formal analysis; Investigation; Writing - Original draft preparation.

References

[1] P Putra. Preparation of activated carbon from coffee grounds as a supercapacitor electrode: Pembuatan karbon aktif dari ampas kopi sebagai elektroda superkapasitor (*in Indonesian*). *Sunan Kalijaga Journal of Physics* 2025; **7(1)**, 1-6.

[2] CH Wang, WC Wen, HC Hsu and BY Yao. High-capacitance KOH-activated nitrogen-containing porous carbon material from waste coffee grounds in supercapacitor. *Advanced Powder Technology* 2016; **27(4)**, 1387-1395.

[3] R Farma, RI Julita, I Apriyani, A Awitdrus and E Taer. $ZnCl_2$-assisted synthesis of coffee bean bagasse-based activated carbon as a stable material for high-performance supercapacitors. *Materials Today: Proceedings* 2023; **87**, 25-31.

[4] O Khadka, U Lawaju, S Koju, RC Rai, ML Nakarmi and P Joshi. Activated carbon derived from coffee waste as supercapacitor electrode material. *Scientific World* 2024; **17(17)**, 19-26.

[5] S Mukhiemer, A Daraghmah, H Nassar, S Hussain, H Lim, H Han, TW Kim and HS Hilal. Physically and chemically activated carbon from coffee waste in high performance supercapacitor electrodes. *Physical Sciences* 2024. https://doi.org/10.20944/preprints202410.0924.v1

[6] M Marpongahtun, AH Siregar, AR Liandi, A Daulay, S Salmiati, AS Prayugo and R Annisa. A

green approach to N, S-doped carbon dots from Jengkol peel (*Archidendron pauciflorum*) for ratiometric sensing of Amaranth dye. *Trends in Sciences* 2025; **22(9)**, 10340.

[7] K Pandey and HK Jeong. Coffee waste-derived porous carbon based flexible supercapacitors. *Chemical Physics Letters* 2022; **809**, 140173.

[8] M Biegun, A Dymerska, X Chen and E Mijowska. Study of the active carbon from used coffee grounds as the active material for a high-temperature stable supercapacitor with ionic-liquid electrolyte. *Materials* 2020; **13(18)**, 3919.

[9] TX Shang and XJ Jin. Waste particleboard-derived nitrogen-containing activated carbon through KOH activation for supercapacitors. *Journal of Solid State Electrochemistry* 2016; **20(7)**, 2029-2036.

[10] C Yang, Y Liu, C Ma, M Norton and J Qiao. Preparing desirable activated carbons from agricultural residues for potential uses in water treatment. *Waste and Biomass Valorization* 2015; **6(6)**, 1029-1036.

[11] C Lu, Z Yu, X Zhang and X Ma. $ZnCl_2$-KOH modulation of biomass-derived porous carbon for supercapacitors. *Energy Sources, Part A: Recovery, Utilization, and Environmental Effects* 2024; **46(1)**, 2212-2222.

[12] J Li, K Han, D Wang, Z Teng, Y Cao, J Qi, M Li and M Wang. Fabrication of high performance structural N-doped hierarchical porous carbon for supercapacitors. *Carbon* 2020; **164**, 42-50.

[13] D Tang, L Lu, Z Luo, B Yang, J Ke, W Lei, H Zhen, Y Zhuang, J Sun, K Chen and J Sun. Heteroatom-doped hierarchically porous biochar for supercapacitor application and phenol pollutant remediation. *Nanomaterials* 2022; **12(15)**, 2586.

[14] R Hossain, RK Nekouei, I Mansuri and V Sahajwalla. *In-situ* O/N-heteroatom enriched activated carbon by sustainable thermal transformation of waste coffee grounds for supercapacitor material. *Journal of Energy Storage* 2021; **33**, 102113.

[15] S Hussain, A Oyebade, MR Hossain, F Abbas and N Siraj. Carbon-based anode materials for metal-ion batteries: Current status, challenges, and future directions. *Batteries* 2025; **11(12)**, 444.

[16] Y Wang, T Liu, X Lin, H Chen, S Chen, Z Jiang, Y Chen, J Liu, J Huang and M Liu. Self-templated synthesis of hierarchically porous N-doped carbon derived from biomass for supercapacitors. *ACS Sustainable Chemistry & Engineering* 2018; **6(11)**, 13932-13939.

[17] R Jangra, P Mahendia, M Karakoti, NG Sahoo, A Srivastava, OP Sinha, TD Clemons, U Deshpande and S Mahendia. $ZnCl_2$-assisted conversion of nitrogen-containing biomass carbon from marigold flower: Toward highly porous activated nitrogen-doped carbon for low ESR and enhanced energy density supercapacitors. *Journal of Energy Storage* 2024; **75**, 109728.

[18] R Sharma, M Khalid and MY Ismail. Enhancing surface properties of circular carbon biochar derived from spent coffee beans through $ZnCl_2$/KOH activation. *BioEnergy Research* 2024; **18(1)**, 2.

[19] Y Ma. Comparison of activated carbons prepared from wheat straw via $ZnCl_2$ and KOH activation. *Waste and Biomass Valorization* 2017; **8(3)**, 549-559.

[20] Y Wan, Y Hu and W Zhou. Catalytic mechanism of nitrogen-doped biochar under different pyrolysis temperatures: The crucial roles of nitrogen incorporation and carbon configuration. *Science of The Total Environment* 2022; **816**, 151502.

[21] P Simon and Y Gogotsi. Materials for electrochemical capacitors. *Nature Materials* 2008; **7(11)**, 845-854.

[22] TE Rufford, D Hulicova-Jurcakova, Z Zhu and GQ Lu. Nanoporous carbon electrode from waste coffee beans for high performance supercapacitors. *Electrochemistry Communications* 2008; **10(10)**, 1594-1597.

[23] TE Rufford, D Hulicova-Jurcakova, E Fiset, Z Zhu and GQ Lu. Double-layer capacitance of waste coffee ground activated carbons in an organic electrolyte. *Electrochemistry Communications* 2009; **11(5)**, 974-977.

[24] Z Geng, Q Xiao, D Wang, G Yi, Z Xu, B Li and C Zhang. Improved electrochemical performance of biomass-derived nanoporous carbon/sulfur composites cathode for lithium-sulfur batteries by

nitrogen doping. *Electrochimica Acta* 2016; **202**, 131-139.

[25] SG Kandalkar, DS Dhawale, CK Kim and CD Lokhande. Chemical synthesis of cobalt oxide thin film electrode for supercapacitor application. *Synthetic Metals* 2010; **160(11-12)**, 1299-1302.

[26] S Ye, J Feng and P Wu. Deposition of three-dimensional graphene aerogel on nickel foam as a binder-free supercapacitor electrode. *ACS Applied Materials & Interfaces* 2013; **5(15)**, 7122-7129.

[27] J Choi, C Zequine, S Bhoyate, W Lin, X Li, P Kahol and R Gupta. Waste coffee management: Deriving high-performance supercapacitors using nitrogen-doped coffee-derived carbon. *C* 2019; **5(3)**, 44.

[28] P Yuan, J Mo, X Sha, X Liu, L Xiao and G Chen. Temperature-modulated nitrogen-doped porous carbon derived from coffee grounds as an anode for high-performance lithium-ion batteries. *Diamond and Related Materials* 2025; **152**, 111921.

[29] V Thithai, X Jin, MA Ahmed and JW Choi. Physicochemical properties of activated carbons produced from coffee waste and empty fruit bunch by chemical activation method. *Energies* 2021; **14(11)**, 3002.

[30] VN Toan, DHM Nguyen, LH Minh, HN Tran, TTA Hoa, STH Thai, LTM My, TP Nguyen, PT Trung and VTT Ho. High surface of activated carbon derived from waste coffee sludge by hydrothermal process at low temperature, Available at: https://papers.ssrn.com/sol3/papers.cfm?abstract_id=5222533, accessed January 2026.

[31] Q Jiang, Z Zhang, S Yin, Z Guo, S Wang and C Feng. Biomass carbon micro/nano-structures derived from ramie fibers and corncobs as anode materials for lithium-ion and sodium-ion batteries. *Applied Surface Science* 2016; **379**, 73-82.

[32] C Choi, SD Seo, BK Kim and DW Kim. Enhanced lithium storage in hierarchically porous carbon derived from waste tea leaves. *Scientific Reports* 2016; **6(1)**, 39099.

[33] A Das, S Pisana, B Chakraborty, S Piscanec, SK Saha, UV Waghmare, KS Novoselov, HR Krishnamurthy, AK Geim, AC Ferrari and AK Sood. Monitoring dopants by Raman scattering in an electrochemically top-gated graphene transistor. *Nature Nanotechnology* 2008; **3(4)**, 210-215.

[34] DNKP Negara, IM Widiyarta, IGAK Suriadi, IGK Dwijana, IMDB Penindra, IGNPT Tenaya, IGK Sukadana and AS Ferdinand. Development of mesoporous activated carbons derived from brewed coffee waste for CO2 adsorption. *EUREKA: Physics and Engineering* 2023; **2**, 17-27.

[35] HS Karapınar. Adsorption performance of activated carbon synthesis by $ZnCl_2$, KOH, H_3PO_4 with different activation temperatures from mixed fruit seeds. *Environmental Technology* 2022; **43(9)**, 1417-1435.

[36] TX Shang, RQ Ren, YM Zhu and XJ Jin. Oxygen- and nitrogen-co-doped activated carbon from waste particleboard for potential application in high-performance capacitance. *Electrochimica Acta* 2015; **163**, 32-40.

[37] H Chen, H Wei, N Fu, W Qian, Y Liu, H Lin and S Han. Nitrogen-doped porous carbon using $ZnCl_2$ as activating agent for high-performance supercapacitor electrode materials. *Journal of Materials Science* 2018; **53(4)**, 2669-2684.

[38] Q Abbas, R Raza, I Shabbir and AG Olabi. Heteroatom doped high porosity carbon nanomaterials as electrodes for energy storage in electrochemical capacitors: A review. *Journal of Science: Advanced Materials and Devices* 2019; **4(3)**, 341-352.

[39] N Chalmpes, I Tantis, AW Alsmaeil, BS Aldakkan, A Dimitrakou, MA Karakassides, CE Salmas and EP Giannelis. Elevating waste biomass: Supercapacitor electrode materials derived from spent coffee grounds. *Energy & Fuels* 2025; **39(2)**, 1305-1315.

[40] YH Chiu and LY Lin. Effect of activating agents for producing activated carbon using a facile one-step synthesis with waste coffee grounds for symmetric supercapacitors. *Journal of the Taiwan Institute of Chemical Engineers* 2019; **101**, 177-185.

[41] E del Ángel Meraz and AP Aguirre. Supercapacitors for storing energy from coffee bean waste. *Renewable Energy, Biomass & Sustainability* 2020; **2(2)**, 7-15.

[42] JW Lee, AS Hall, JD Kim and TE Mallouk. A facile and template-free hydrothermal synthesis of Mn_3O_4 nanorods on graphene sheets for supercapacitor electrodes with long cycle stability. *Chemistry of Materials* 2012; **24(6)**, 1158-1164.

[43] H Wang, Z Zhang, Y Li, D Pei, S Wan, Y Li and H Lu. Facile fabrication of N-doped carbon derived from kiwi fruit peel for advanced supercapacitor. *Academic Journal of Science and Technology* 2023; **4(2)**, 78-82.

[44] W Li, D Chen, Z Li, Y Shi, Y Wan, J Huang, J Yang, D Zhao and Z Jiang. Nitrogen enriched mesoporous carbon spheres obtained by a facile method and its application for electrochemical capacitor. *Electrochemistry Communications* 2007; **9(4)**, 569-573.

[45] H Chen, F Sun, J Wang, W Li, W Qiao, L Ling and D Long. Nitrogen doping effects on the physical and chemical properties of mesoporous carbons. *The Journal of Physical Chemistry C* 2013; **117(16)**, 8318-8328.

[46] Y Zhao, L Huang and G Sun. Preparation of high-performance KOH-activated biochar from agricultural waste (Sapindus mukorossi) and its application in organic dye removal. *Sustainability* 2025; **17(19)**, 8674.

[47] C Schneidermann, C Kensy, P Otto, S Oswald, L Giebeler, D Leistenschneider, S Grätz, S Dörfler, S Kaskel and L Borchardt. Nitrogen-doped biomass-derived carbon formed by mechanochemical synthesis for lithium-sulfur batteries. *ChemSusChem* 2019; **12(1)**, 310-319.